Effect of Micelle Formation on Chromatographic Movement of Surfactant Mixtures

Solutions are presented for equations which describe the chromatographic transport of binary surfactant mixtures. The formation of micelles in the bulk fluid is taken into account. The effects of micellization on the behavior of surfactant pulses are illustrated by solutions for specific cases. Schemes are presented for offsetting the tendency of surfactant pulses to undergo chromatographic separation because of preferential adsorption of the surfactants on the solid substrate. These schemes take advantage of the effects of micelle formation. Generalizations for n-component surfactant systems are outlined.

J. H. HARWELL,
F. G. HELFFERICH
and
R. S. SCHECHTER

Dept. of Chemical Engineering
The University of Texas at Austin
Austin, TX 78712

SCOPE

Enhanced oil recovery processes which use surfactants to decrease the interfacial tension between water and oil to a level sufficient to release trapped oil drops have now been tested extensively in the laboratory and to some extent in the field (Lake and Pope, 1979). The technology has improved rapidly and commercial application now appears feasible. One potential difficulty, however, is the chromatographic separation of constituents blended to form the micellar (surfactant-rich) solution. Various surfactant types, different isomers of the same surfactant and cosurfactants are often blended in an electrolyte solution designed to optimize oil recovery. If any one of the constituents of this micellar solution becomes separated from the others as they flow through the oil-bearing formation, the oil recovery efficiency will be impaired. The separation may occur by any one or a combination of mechanisms. For example, during the displacement process a number of fluid phases may coexist at various positions within the formation. Since these phases generally move at different velocities, selective partitioning of one constituent relative to the others can lead to separation.

A second possibility, and the one considered here, is chromatographic separation due to selective adsorption of constituents onto reservoir minerals. If several of the constituents are surfactants then the nature and degree of separation is greatly complicated by their tendency to form mixed micelles (Clint, 1975; Rubingh, 1978). Trogus, et al, 1979a recognized the need to account for the presence of mixed micelles and have considered the chromatographic separation attending the continuous injection (infinite slug) of a two-component surfactant mixture into a porous medium. The flow system was considered to be linear and homogeneous and the fluids single phase, thus excluding the presence of oil. They also assumed without proof that the waves would be self-sharpening so that wave velocities and compositions could be determined by integral material balances. An adsorption model (called here the Trogus Model) which exhibits all of the essential features of the complex isotherm behavior associated with adsorption of mixed surfactants from aqueous solution (Trogus, Wade, Schechter, 1979b) was used in the analysis.

The Trogus adsorption model is also used here. Those features of the model needed to interpret the results are described. Further details are reported elsewhere (Trogus, Wade, Schechter, 1979b). This is followed by a discussion of the Helfferich approach applied to the problem of chromatographic separation of surfactants. This theory is complex and no attempt is made to justify it nor explain it fully here. The interested reader is referred to the book by Helfferich and Klein, 1970.

The purpose of the present work is to examine the chromatographic separation of surfactants under more general initial and boundary conditions using a theory of multicomponent chromatography developed by Helfferich and Klein, 1970, which yields a general solution of the problem, permitting examination of finite slugs as well as of injection sequences of different surfactant solutions. Furthermore it will be shown that the ad hoc assumptions imposed by Trogus et al, 1979a can be justified. In addition a wide range of adsorption parameters will be considered and the results extended to an arbitrary number of surfactant components.

The results of the calculations can conveniently be divided into three sections. First, composition path diagrams for binary surfactant mixtures are presented. These are laid down once and for all, permitting the consideration of chromatographic effects attending an arbitrary sequence of fluid injections without further calculation. Therefore, the topological features of these diagrams are of general importance and are considered first.

The next section considers a variety of injection sequences. The greatest attention is given to the propagation of a square-wave surfactant pulse (surfactant slug) since most enhanced oil recovery processes utilize a slug of small size (relative to the pore volume). In the last section the results are extended to multicomponent systems.

CONCLUSIONS AND SIGNIFICANCE

This study points to new, general features of the chromatographic separation of micellar solutions. One of the most striking is the discovery of indifferent concentration waves which move with the fluid velocity, indicating no interaction with the substrate. The conditions for the existence of such waves are shown to be quite general, making their existence in real solutions likely. Since these calculations do not include the effects of oil, they can not be considered to be truly representative of actual processes. However, they do provide important practical guidelines indicating, for example, that small high-concentration slugs may be preferable to large low-concentration slugs. It is also suggested that the tendency of the surfactant mixture to undergo chromatographic separation because of selective adsorption can be prevented by the use of a surfactant preflood with the same monomer concentration as the surfactant slug.

F. G. Helfferich is presently with the Dept. of Chemical Engineering, Pennsylvania State University, University Park, PA 16802.

ISSN-0001-1541-82-5664-0448-$2.00.

TROGUS ADSORPTION MODEL

Amphiphilic molecules which have distinct hydrophilic and lipophilic moieties tend to exhibit a considerable degree of intermolecular organization when dissolved in aqueous solutions. They tend to aggregate forming regions consisting of a hydrophobic core (not necessarily spherical) surrounded by a hydrophilic shell. This process of organization is termed micelle formation and the groups of associated surfactant molecules which are more or less randomly distributed throughout the solution are called micelles. They tend to form at a more or less well defined concentration called the critical micelle concentration (CMC).

Micelles are often small, consisting of aggregates of 10–30 molecules which decompose and reform rapidly. Individual surfactant molecules (called monomer) are distributed throughout the aqueous phase surrounding the micelles. These can, and often do, exchange with aggregated molecules. The micelles and monomer should be visualized as being uniformly distributed throughout the aqueous phase. A chemical analysis of a sample of reasonable size drawn from the solution will reveal the total surfactant concentration. Monomer concentrations must be inferred from experiments distinguishing micelles from monomers.

If the surfactant is a mixture, then individual micelles will be mixed; that is, each will contain surfactant of all types present in the solution. The composition of surfactant in the micelles will differ from the composition of monomer. It will be assumed here that the monomer is in equilibrium with the micelles.

It has been established that surfactant adsorption depends on the monomer composition and concentration and not on the total solution concentration (Fernandez, 1978). Interesting and unexpected isotherm behavior may occur (Trogus, Wade, Schechter, 1979b) attending adsorption from mixed surfactant solutions. The observed phenomena, such as apparent adsorption maxima and minima, are predicted by a simplified model, the Trogus model, which imposes the following assumptions:

(a) The composition and concentration of surfactant in the monomer and in the micelles can be approximated by assuming that these are separate phases in thermodynamic equilibrium.

(b) Micelles do not adsorb and adsorption, therefore, is a function of monomer concentration and composition only.

(c) Adsorption of an individual surfactant component is a linear function of its monomer concentration (Henry's Law) and is independent of micelle concentration and of the concentrations of the other molecules present as monomer.

The "phase separation model" according to (a) is generally used to describe the monomer-micellar equilibrium of a single surfactant species. The model predicts that micelles form at a well defined concentration (CMC) rather than over a range of concentrations and that the monomer concentration remains constant for all solution concentrations beyond the CMC. This is, of course, an approximation and a more rigorous treatment requires use of the laws of mass action. Thus, surfactants associate with each other to some extent at concentrations lower than the CMC and micelles continue to change in both average aggregation number, distribution of aggregation numbers and morphology as the surfactant concentration is increased. However, most experiments indicate that micelles form over a small range of surfactant concentration and that the phase separation model is an excellent approximation.

To treat mixed micelles, Mysels and Otter, 1961, assumed that the separate micellar phase is ideal. They also invoked the validity of an empirical equation relating the CMC to the electrolyte concentration to develop the following expression

$$\frac{c_{i,m}}{c_{j,m}} = \frac{c_{i,d}}{c_{j,d}}\left(\frac{c_j^*}{c_i^*}\right)^{\theta} \quad \begin{matrix} i = 1,2,\ldots,n \\ j = 1,2,\ldots,n \\ i \neq j \end{matrix} \tag{1}$$

where $c_{i,m}$ is concentration of surfactant species i in the micellar phase expressed as moles per volume of solution, $c_{i,d}$ is the monomer concentration of component i also expressed as moles per volume of solution, c_i^* is the pure component CMC and θ is an empirical constant. The concentrations $c_{i,m}$ and $c_{i,d}$ are defined so that

$$c_i = c_{i,m} + c_{i,d} \tag{2}$$

where c_i is the total concentration of species i. It should also be noted that c_i^* is the CMC of species i measured in the absence of the other species. The CMC of a mixture is a function of the concentration c_i. It is given by (Trogus, Wade, Schechter, 1979b):

$$c_d = \left[\frac{(\Pi c_i^*)^{\theta}}{\sum x_i \left(\prod_{i \neq j} c_j^*\right)^{\theta}}\right]^{1/\theta} \quad i = 1,2,\ldots,n \tag{3}$$

where c_d is the CMC of the mixture given by the sum of monomer concentrations, and x_i is the monomer mole fraction of component i. Thus

$$c_d = \sum c_{i,d} \qquad i = 1,2,\ldots,n \tag{4}$$

Fernandez, 1978 studied the adsorption of an isomerically pure suite of alkyl benzene sulfonates and found that a plateau adsorption was attained at the CMC. This is not to preclude the possibility that surfactant aggregates are formed on the substrate. Indeed, it appears that lateral interactions are an important feature of surfactant adsorption (Scamehorn, 1980). The adsorbate is in equilibrium with the monomer which is in turn in equilibrium with the micellar phase. Thus assumptions (a) and (b) of the Trogus Model are in good agreement with experimental evidence.

Assumption (c) requires that

$$q_i = k_i c_{i,d} \quad i = 1,2,\ldots,n \tag{5}$$

where q_1 is the concentration of the adsorbate expressed as moles adsorbed per gram of solid phase. Equation 5 does not accurately represent the fine structure of the adsorption isotherm. It is now known that adsorption is both nonlinear and synergistic. However, Trogus et al. (1979b) have shown that this simple adsorption model predicts, by solving Eqs. 1, 2, 3, 4, and 5 simultaneously, complex isotherm shapes giving rise to apparent adsorption maxima and minima and to a dependence of the (pseudo-single component) "isotherm" on the ratio of solid to liquid in static experiments. All of these phenomena have been observed. Thus the Trogus Model represents the gross features of surfactant adsorption, even though it fails to provide a precise representation of the fine structure. It is therefore expected that the features of chromatographic transport predicted here will be unaltered when Eq. 5 is replaced by more accurate expressions.

CHROMATOGRAPHIC PROBLEM

The equations describing chromatographic phenomena are more convenient if concentrations are expressed in terms of a unit column volume. The following variables are thus introduced and defined:

$$C_i^* = \phi c_i^*$$

$$C_i = \phi c_i$$

$$C_{i,d} = \phi c_{i,d}$$

$$C_{i,m} = \phi c_{i,m}$$

$$\overline{C}_i = (1 - \phi)\hat{\rho}_s q_i$$

The component material balance equations will be written in terms of these variables. Note that

$$\overline{C}_i = K_i C_{i,d}$$

where

$$K_i = \frac{k_i(1 - \phi)\rho_s}{\phi}$$

The chromatographic column is assumed to be one-dimensional and uniform, and a single mobile fluid phase is assumed to be in equilibrium with an immobile adsorbate. If the average fluid ve-

locity is taken to be a constant, and if dispersion is neglected, then a material balance for component i is

$$\frac{\partial C_{i,T}}{\partial t} + V\frac{\partial C_i}{\partial z} = 0 \quad i = 1,2,\ldots,n \tag{6}$$

where

$$C_{i,T} = \bar{C}_i + C_i$$

The associated initial and boundary conditions are, for infinite slugs

$$C_i = C_{i,0} \qquad t = 0, z \geq 0 \tag{7}$$

$$C_i = C_{i,\text{in}} \qquad t > 0, z = 0 \tag{8}$$

Those for finite slugs (consecutive injection of two different fluids) are

$$C_i = C_{i,0} \qquad t = 0, z \geq 0 \tag{9}$$

$$C_i = C_{i,\text{in}} \qquad 0 \leq t < \Delta t, z = 0 \tag{10}$$

$$C_i = C'_{i,\text{in}} \qquad t \geq \Delta t, z = 0 \tag{11}$$

METHOD OF SOLUTION

The solution of the above equations was obtained by application of the Helfferich theory of multicomponent, multiphase displacement in porous media (Helfferich, 1981; Helfferich and Klein, 1970). The basis of the Helfferich theory is the recognition that the solution of equations of the above type will be in terms of waves whose composition and velocity make them propagationally stable. The theoretical statement of this fact is called the "coherence condition." The coherence condition may be stated mathematically as follows. In a propagationally stable (coherent) wave, it must be true that

$$V_{c1} = V_{c2} = \ldots = V_{cn} \tag{12}$$

where

$$V_{c_i} = (\partial z/\partial t)_{c_i} \qquad i = 1,2,\ldots,n \tag{13}$$

and V_{c_i} is the velocity at which a given concentration value C_i advances in the direction of flow. The key step in the application of the Helfferich theory is the use of the coherence condition to construct a composition path grid. The composition paths are curves in the coordinate space of the dependent variables—here taken as the total fluid phase concentrations, C_i—corresponding to variations which are coherent. For a system with given equilibrium and flow properties (Eqs. 1 to 5) a unique grid of such paths can be constructed and then applied to any initial and boundary conditions. The results obtained from a specific application (e.g., Eqs. 9 through 11) are not only the number and composition of propagationally stable waves, the velocities of these waves, and the results of wave-wave interactions, but also whether these waves are self-sharpening, indifferent, or spreading.

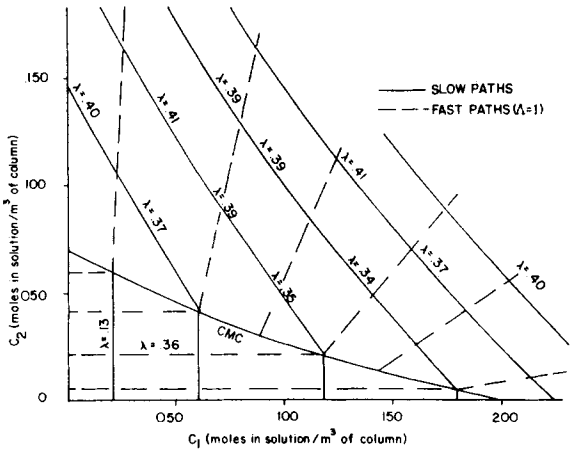

Figure 1. Composition path grid for a typical Trogus system. Concentrations near the CMC. Parameter values presented in Table 1.

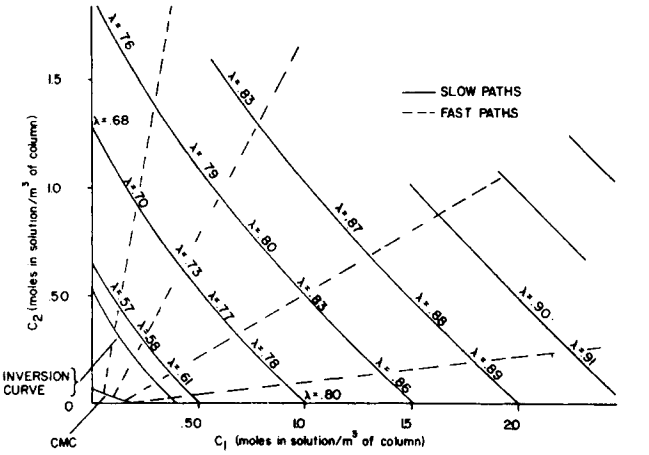

Figure 2. Composition path grid for a typical Trogus system. Concentrations far from the CMC. Parameter values presented in Table 1.

TABLE 1. PARAMETER VALUES USED TO GENERATE COMPOSITION PATH GRID IN FIGURES 1 AND 2

$C_1^* = 1.0\ \text{mol/m}^3$
$C_2^* = 0.35\ \text{mol/m}^3$
$\theta = 1.8$
$k_1 = 0.21 \times 10^{-3}\ \text{m}^3/\text{kg}$
$k_2 = 0.80 \times 10^{-3}\ \text{m}^3/\text{kg}$
$\hat{\rho}_s = 2.1 \times 10^{-3}\ \text{kg/m}^3$
$\phi = 0.2$

The composition path grid for a typical two-component Trogus system is presented in Figures 1 and 2. The parameter values chosen for the specific system are presented in Table 1. The numbers appearing on the curve are the eigenvelocities, that is, the eigenvalues λ related to the velocities of the respective compositions in coherent waves by

$$\lambda = V_{\text{wave}}/V \tag{14}$$

where V is the bulk fluid velocity and V_{wave} the velocity of the coherent wave defined by Eq. 13. The construction of composition path grids, and the method of determining the number of waves and their compositions and velocities for specific initial and boundary conditions, are discussed in detail in reference (Helfferich and Klein, 1970). The mathematical details of the application to multiphase flow in porous media are presented in reference (Helfferich, 1981).

CHARACTERISTIC FEATURES OF TROGUS MODEL

The effects of micelles on the chromatographic flow of surfactant mixtures may be observed in the characteristic features of the composition path grids of a typical Trogus system (Figures 1 and 2). Below the CMC the grid is strictly orthogonal, and no wave-wave interference can occur. All waves arising from compositions below the CMC are indifferent waves. These features below the CMC are determined entirely by the adsorption model (constant Henry's Law coefficients) and so may not be characteristic of real systems.

Above the CMC one family of composition paths is linear. The eigenvelocity along these paths is always unity. Compositions on the composition path grid connected by one of these paths will produce a coherent wave that propagates at the bulk fluid velocity. Such a wave will arise only when the column ahead of and behind the wave contains both surfactants at concentrations at or above

the CMC. These waves are entirely and exclusively variations of micelle concentration, at constant micelle composition.

Monomer concentrations also do not vary across such waves. This feature is not dependent on the choice of adsorption isotherm but, rather, upon the phase separation model and the assumption that only the monomeric form of the surfactant adsorbs. Thus, the unit-velocity paths are loci of constant monomer composition along which only the concentration of micelles in equilibrium with the monomers varies. This is analogous to adding liquid to a two-phase vapor-liquid mixture which is at equilibrium. If the liquid added is of the same composition as the liquid already present, then the total volume of the system can increase without change in either the amount or composition of the vapor. Since the phase separation model is generally agreed to be a good approximation of surfactant behavior at high aggregation numbers, the behavior resulting from the unit-velocity paths is expected to be physically real.

That these waves will travel at the velocity, V, of the bulk fluid can be shown as follows. The wave velocity, V_{wave}, from Eqs. 13 and 6 is found to be

$$V_{\text{wave}} = (\partial z/\partial t)_{C_i} = \frac{V}{1 + (\partial \bar{C}_i/\partial t)_z/(\partial C_i/\partial t)_z} \qquad (15)$$

Since the monomer concentrations do not vary along the paths, neither do the adsorbed concentrations, $\bar{C}_i$. Thus, $V_{\text{wave}} = V$. Moreover, since this argument applies to all surfactant components i, the coherence condition (Eq. 12) is obeyed along the loci.

If a column contains compositions above the CMC, the coherent waves that arise may be self-sharpening, indifferent, or spreading. The procedure for determining the number, composition, and behavior of the waves arising from a specific set of initial and boundary conditions will be illustrated. To determine the system's behavior, the initial and boundary conditions are first located on the composition path grid (for example, Figures 3 a1, a2). Since these compositions are not connected by a single composition path, the situation generated by the injection is initially noncoherent. Only coherent waves are propagationally stable, so the single noncoherent wave generated by injection will break up into coherent waves. To determine the composition and number of these waves, the first step is to construct a "route" on the composition path grid that connects the injected and initial conditions. This route must be exclusively along composition paths. Since the slower coherent wave advances the lesser distance through the column, the route, beginning from the injected composition, follows a slow path first and then switches to the fast path leading to the point which corresponds to the initial composition. The point of intersection of the slow and fast paths is the composition of the intermediate zone that will arise between the two waves (composition B in Figure 3 a1). After the construction of the initial route, one must determine if it will be followed exactly. The first step is to determine if the waves are self-sharpening, spreading, or indifferent. If the eigenvelocity decreases along a path in the direction of flow, then the wave will be self-sharpening; if the eigenvelocity is constant along the path, the wave will be indifferent; if increasing, the wave will be spreading. Only if the wave is self-sharpening may the system not follow the composition route exactly. The self-sharpening wave is a shock wave. The discontinuity across a shock front cannot be described by the differential relations used to construct the composition path grid. In that case, an integral material balance across the shock and a trial and error procedure must be used to determine the composition of the intermediate zone and the velocity of the shock. (See appendix.) However, in most cases the composition will be close to that found from the initial route construction. An example where this is not true is seen in case 4. Here, the discontinuity at the CMC causes the actual route to differ markedly.

The waves set up by the injection of a "drive" following the slug are determined in the same manner. This time, the route connects the composition injected behind the slug with the slug composition. Once again, case 1, Figures 3 a1 and 3 a2, serve as an illustration. After these waves have been determined as to composition and velocity, their interactions can be plotted on a distance-time diagram (Figures 3 b). The results of wave-wave interactions are determined by locating the compositions of the interfering waves on the composition path grid and again following the above procedure. That is, when a fast wave from a later injection catches up (interferes) with a slow wave from an earlier injection, a local and

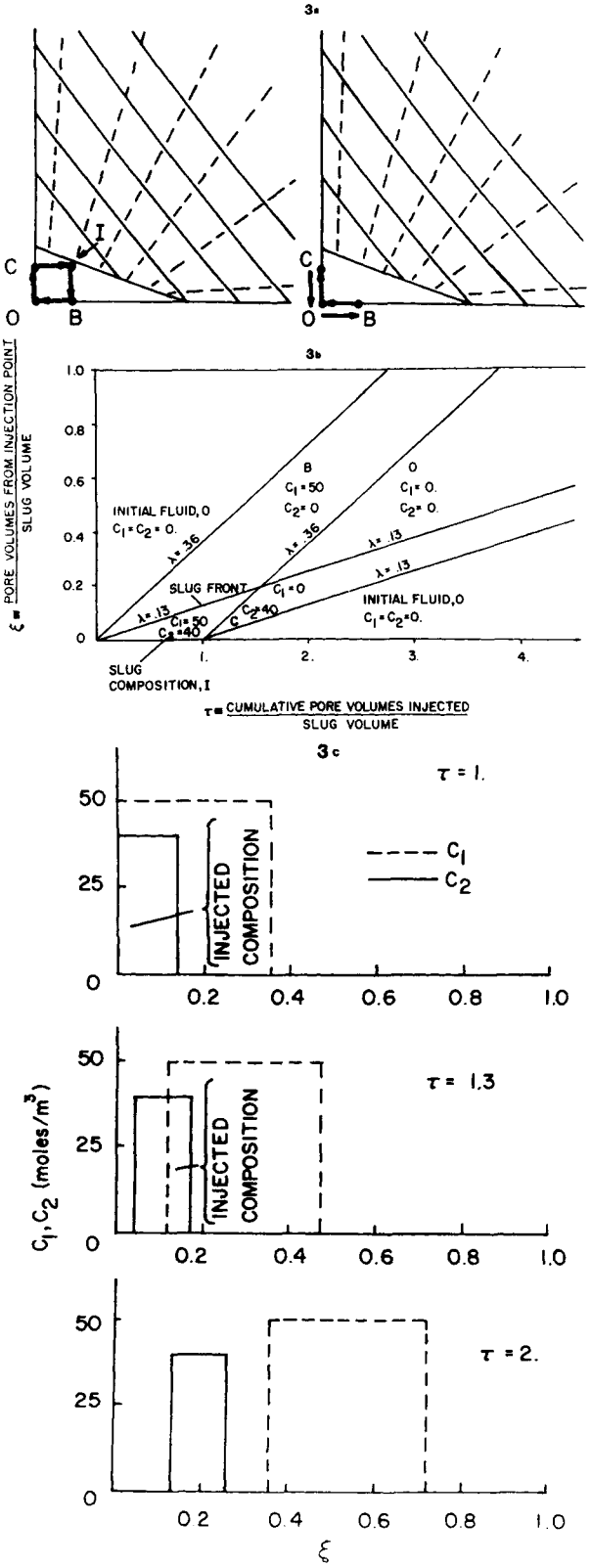

Figure 3. Behavior of a Trogus system in the absence of micelle formation. The behavior is typical of low concentration systems such as seen in the use of liquid chromatography as an analytic tool. (a) Schematic of composition route development (b) Distance-time diagram (c) Column profiles.

temporary noncoherence is created; this noncoherence then acts as the origin of new coherent waves, in exactly the same manner as does a noncoherence at the injection point.

The following generalizations may be made concerning behavior of the waves in a Trogus system. When the column ahead of a slug is devoid of surfactant, the slug composition is above the CMC, and the drive is devoid of surfactant, the waves generated by slug injection, two in number, will be self-sharpening. Thus, the assumption of Trogus et al. (1979a) that waves in a Trogus-type system are self-sharpening is valid for initial conditions of zero surfactant concentrations and infinite slugs. Before any wave-wave interactions occur, all the waves generated at the back of finite slugs by drive injection, under the above stated conditions, will be indifferent waves. The fastest of these waves will have an eigenvelocity of unity—it will move at the bulk fluid velocity, and the micelle concentration will be zero on its upstream side. The result is that when the ratio of slug volume to pore volume is small enough, micelles disappear from the system. This prediction is discussed further below. After interference, waves may be self-sharpening, spreading, or indifferent.

Another feature of a two-component Trogus system is the existence of what has here been termed an "inversion curve." The inversion curve is the locus of points, in the composition space, for which $\bar{C}_1/C_1 = \bar{C}_2/C_2$. Its existence is dependent upon the occurrence of micellization and upon the following inequalities:

$$C_1^* > C_2^* \tag{16}$$

$$K_1 < K_2 \tag{17}$$

Near the CMC (Figure 1), the eigenvalues along the slow paths (the curved paths) decrease in the direction of increasing concentration of component 1. In Figure 2, above the inversion curve, the eigenvelocities increase in that direction. Along the inversion curve itself the eigenvelocities are constant. The physical significance of the inversion curve is as follows. If a fluid with composition above the CMC but below the inversion curve is injected into a column initially devoid of surfactant, component 1 will emerge first at a concentration above its injected concentration. This phenomena is illustrated in case 2 below. If a fluid with a composition above the inversion curve is injected into the column, component 2 will emerge first and does so at a concentration above its injected concentration. This phenomenon is illustrated in case 3 below. Injection of a fluid with a concentration on the inversion curve into a column devoid of surfactant will produce only one wave: both concentrations will emerge simultaneously at their injected concentrations.

The reason for this behavior may be explained in physical terms. Its occurrence depends upon the component with the larger Henry coefficient also being the component which is preferentially incorporated into the micelles (component 2 in this case). At concentrations between the CMC and the inversion curve, the effects of micellization are not enough to offset the fact that component 2, by virtue of its larger Henry coefficient, is preferentially adsorbed and thus more highly retarded in its progress through the column. But above the inversion curve, enough of component 2 is incorporated into the micelles that, despite its larger Henry coefficient, it is less strongly retarded than component 1. If the component having the largest Henry coefficient is not also preferentially incorporated into the micelles, no inversion curve can exist and this component will always be more strongly retarded in the column.

Two final observations will be made regarding the eigenvelocities. First, on the slow paths they tend to increase as the distance in composition space from the origin increases. This simply implies that the higher the concentration above the CMC, the more effectively the surfactants are shielded from adsorption, and therefore tend to move through the column more rapidly. As a result, fractionation tends to be less rapid at high concentrations. This is illustrated by case 3 considered below and is the reason that surfactant fractionation for highly concentrated slugs may be too small to be observed (Trogus, Wade, Schechter, 1979a). Small degrees of separation (small differences in λ between slow and fast waves) tend to be obliterated by dispersion and finite mass transfer rates, making their detection even more difficult.

It should be noted that the observations in this section arise from an understanding of how a composition path grid is used to determine system behavior for specific initial and boundary conditions. As this procedure is discussed extensively elsewhere (Helfferich and Klein, 1970), it is only mentioned here. Anyone wishing to verify these observations from Figures 1 and 2 should be familiar with it.

Results of Parametric Studies

Composition path grids were constructed for a wide range of values covering the range of physically realistic values. In all cases it was found that the observations made in the preceding section remained valid. Hence, path grids for other values of the parameters are not presented here.

Behavior of Finite and Infinite Slugs

The particular Trogus system specified by the parameter values in Table 1, and corresponding to the composition path grid of Figures 1 and 2, was solved for a variety of initial and boundary conditions. A summary of the cases solved is presented in Table 2. Composition routes, distance-time diagrams, and concentration-profiles are shown in Figures 3 to 7. These cases are discussed below in terms of the behavior of finite slugs. To each case, except case 4, there is a corresponding infinite slug. The behavior of the infinite slugs is not discussed specifically since they are subsets of the finite slugs and largely self-explanatory.

The units used in the distance-time diagrams were chosen to make clear that these diagrams are universally applicable. Any slug size and slug size-to-reservoir pore volume ratio can be represented on one diagram. The only accommodation necessary is that as the slug volume-to-pore volume ratio increases, less of the diagram actually applies. As an example, consider Figure 3c. The ordinate and abscissa are a dimensionless time and distance, respectively. The dimensionless time is cumulative injected volume/slug vol-

TABLE 2. INITIAL AND BOUNDARY CONDITIONS FOR CASES 1 TO 5, CORRESPONDING TO FIGURES 3 TO 7

Case	*$C_1(z)$ $t = 0$ $z \geq 0$	$C_2(z)$ $t = 0$ $z \geq 0$	$C_1(t)$ $0 < t \leq \Delta t$ $z = 0$	$C_2(t)$ $0 < t \leq \Delta t$ $z = 0$	$C_1(t)$ $t > \Delta t$ $z = 0$	$C_2(t)$ $t > \Delta t$ $z = 0$	Comments	Corresponding Figures
1	0	0	0.050	0.040	0	0	System behavior in the absence of micellization	3a,b,c
2	0	0	0.042	1.15	0	0	Dilute slug behavior. Injected composition between CMC and Inversion Curve	4a,b,c
3	0	0	1.00	1.00	0	0	Concentrated slug behavior. Injected composition above Inversion Curve	5a,b,c
4	0	0	0.042	1.15	0.035	0.053	Use of surfactants drive. Note composition of wave with superficial fluid velocity $\lambda = 1$	6a,b,c
5	0.035	0.053	0.042	1.15	0	0	Use of surfactant preflood. No fractionation of slug occurs	7a,b,c

* All concentrations are expressed in mol/m^3.

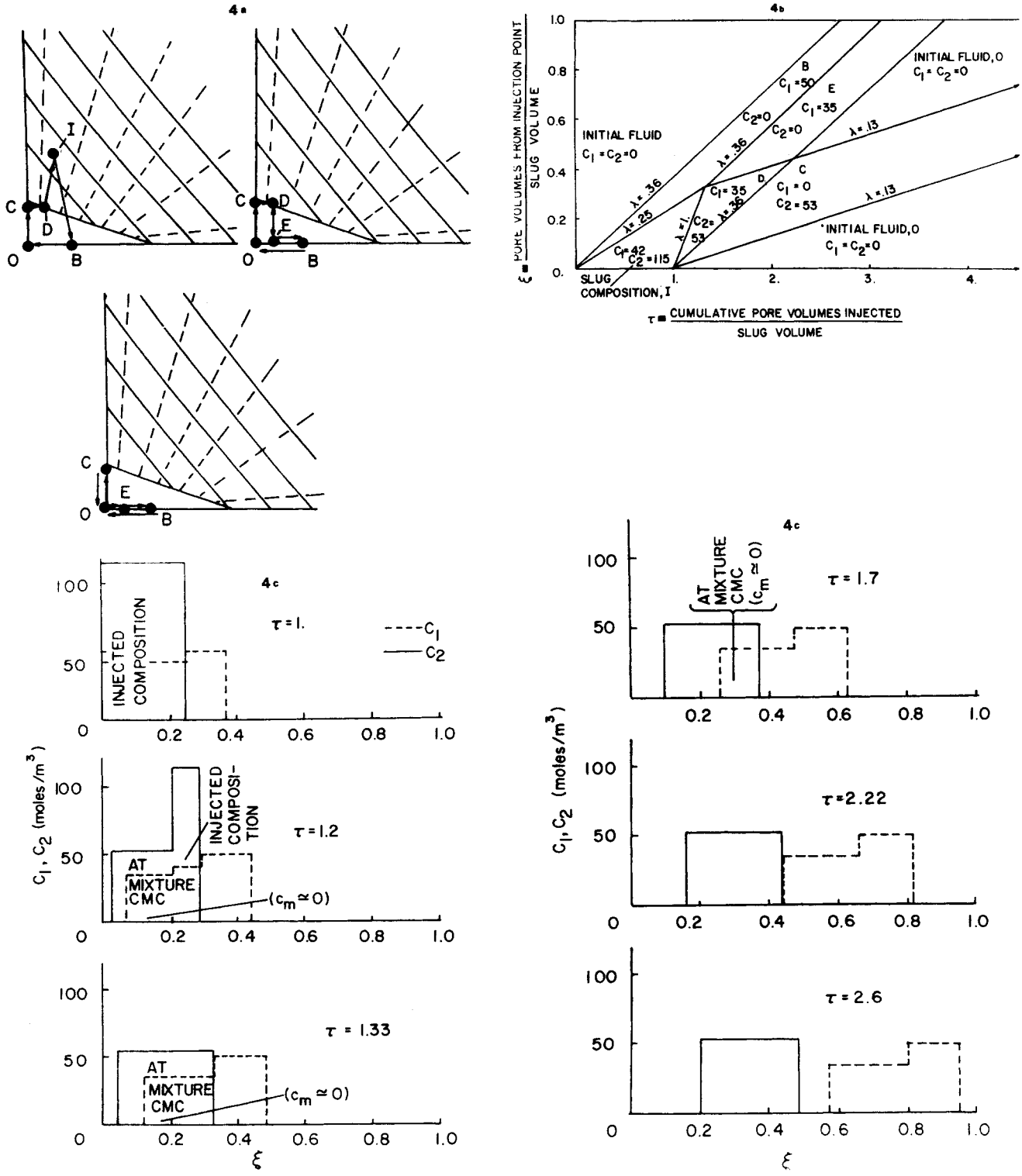

Figure 4. Behavior of a slug of composition between the CMC and the inversion curve. (a) Schematic of composition route development (b) Distance-time diagram (c) Column profiles.

ume. The dimensionless distance from the injection point is in terms of pore volume/slug volume, measured from the injection point. In order to apply a diagram to a specific situation, the slug volume-to-reservoir volume ratio must be specified. Thus, for a slug the size of one pore volume, only that part of the diagram below $\xi = 1$ applies. This is the "distance" to which the reservoir extends. For a slug the size of 0.5 pore volume, all the diagram below $\xi = 2$ applies. Further, for the one-pore-volume slug, a wave moving at the bulk fluid velocity would reach the end of the reservoir ($\xi = 1$) at $\tau = 1$. But for an 0.5 pore volume slug, though a wave of bulk fluid velocity still goes through (1,1) $\xi = 1$ would only be the half-way point in the reservoir.

Case 1: Injected Composition below CMC

Figure 3a shows composition routes for an injected slug composition I followed by a surfactant-free drive. Between the two coherent waves generated at the front of the slug a composition B is established, corresponding to the intersection of the slow path passing through point I (injected composition, slug) with the fast

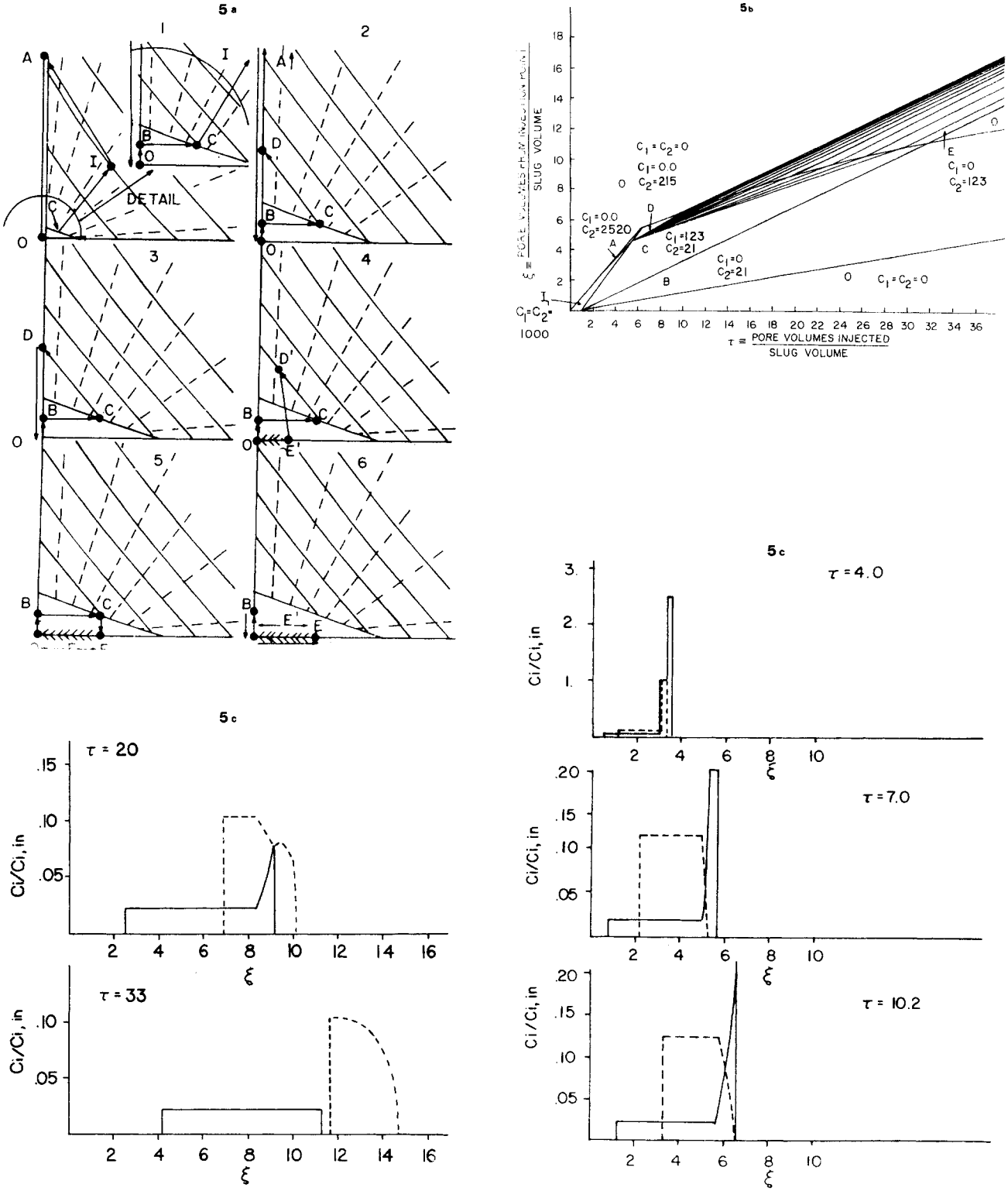

Figure 5. Behavior of a slug of composition above the inversion curve. Preferential incorporation of more strongly adsorbed component into the micellar pseudophase results in counterintuitive behavior described in the test. (a) Schematic of composition route development (b) Distance-time diagram (c) Column profiles.

path passing through point 0 (initial composition of fluid in the column). The diagram indicates that the intermediate zone does not contain component 2. The composition paths resulting from eluting the injected slug with a surfactant-free drive are also shown (OCI), the new intermediate zone between the slow and fast waves at the rear of the slug having the composition C.

To better appreciate the importance of the composition diagram, consider figure 3b which depicts the concentrations as a function of time and distance. The front of the slug propagates slowly ($\lambda = 0.13$). The fast wave at the rear of the slug ($\lambda = 0.36$) catches up with the slow wave at the slug front as shown. Beyond this point in time and space, fluid having the slug composition will no longer exist at any position within the column. The slug in this case decomposes into its components 1 and 2, the latter moving at the lower velocity because $K_2 > K_1$ in this case.

The sequence of events described above correspond, of course,

to the simplest possible case, namely, the chromatographic movement of noninteracting components. To emphasize this point Figure 3c shows profiles at various points in time. The first profile indicates that fluid containing component 1 only has progressed through the column more rapidly, leading the fluid having the injected composition. The second profile considers a point in time after slug injection has been completed. The trailing fluid containing component 2 is now apparent. Finally the two surfactants have been separated. As noted, this sequence is typical of simple chromatographic separations. A sequence of this type will be found for all injected composition below the CMC curve.

Case 2: Injected Compositions between CMC and Inversion Curve

If the slug composition is at I shown in Figure 4a, new and unexpected features arise. Consider the initial column composition and the composition of the drive fluid are both at point 0. The composition paths are shown. The slow path from I intersecting a fast path through 0 exhibits decreasing λ (Figure 1), indicating a self-sharpening behavior. The calculation of point B, the composition of the intermediate zone, therefore requires application of an integral material balance (Appendix). It is interesting to note that the concentration C_1 at B is larger than the injected concentration at I. From point B to 0 the fast path is indifferent.

At the rear of the slug, three waves are generated. This unusual situation arises because the CMC curve represents a discontinuity in the direction of the fast paths. A slow path from 0 leads us to C. Fast paths from C yield D and I successively. The wave DI travels rapidly with a unit velocity as has been previously discussed. Since both path segments CD and DI are linear, a correction with an integral material balance is not necessary (any two points on a *linear* composition path, calculated from the differential coherence condition also obey the integral coherence condition for shocks and discontinuities).

Figure 4b shows the corresponding distance-time diagram. Note the *rapid* degradation of the slug owing to the advance of the unit-velocity wave. When that wave interferes with the slow wave at the slug front, solution having a composition D is in contact with solution of composition B. This is a noncoherent situation and acts as origin of two new waves. The composition of the intermediate zone between these new waves, E, is then found by applying the usual rule, namely, finding the intersection of a slow path through D with a fast path through B. This new intermediate composition ($C_1 = 0.335$, $C_2 = 0$) is easily found by means of Figure 1 and is shown in Figure 4a. Finally an additional wave interference is shown in Figures 4a and b, but now all of the compositions are on or below the CMC curve and the resulting waves are easily visualized.

Figure 4c shows profiles depicting the various stages of the process. It seems worth noting that the ultimate result is to separate the two surfactants into two distinct pulses each at a concentration less than the CMC. Secondly, the peculiar shape of the leading component 1 pulse after 2.6 slug volumes have been injected is a result of the discontinuous nature of the fast paths at the CMC.

Case 3: Slug Compositions Above Inversion Curve

When the slug composition is above the inversion curve, the wave interactions become still more complex (Figure 5). The initial noncoherence between the injected composition, I, and the initial fluid composition, 0, is resolved into two shocks. The plateau region in between has a concentration A. In contrast to case 2, for which the slug composition was between the CMC and the inversion curve, this plateau zone now contains only component 2. The component with the larger Henry coefficient is retarded to a lesser degree than its companion. As has been noted, this counterintuitive behavior is a result of the preferential incorporation of component 2 into the micelles. Note, also, that the two waves at the slug front are now moving faster than the corresponding waves for a slug below the inversion curve ($\lambda = 0.84$ and 0.82). This means that a longer dimensionless distance will be required for the unit-velocity

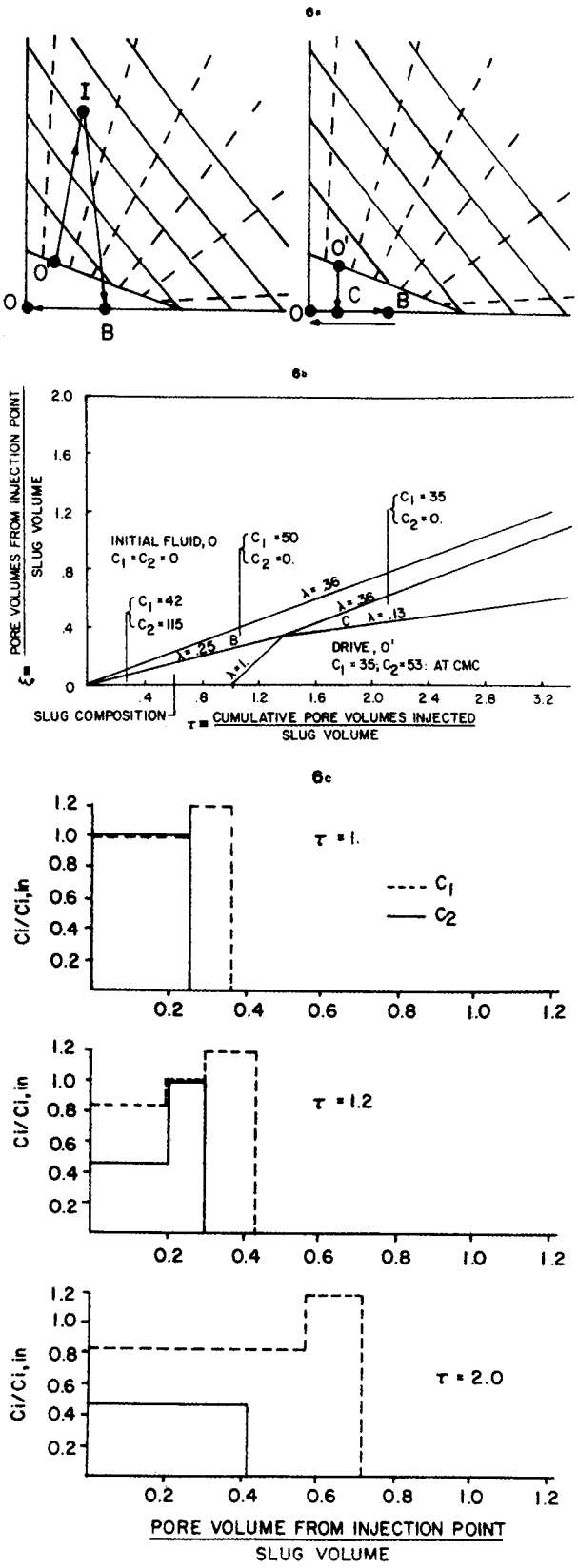

Figure 6. Use of a surfactant drive. Rapid degradation of slug from the rear not prevented. (a) Schematic of composition route development (b) Distance-time diagram (c) Column profiles.

wave produced at the rear of the slug to overtake the wave at the slug front.

When the wave of variation C-I interferes with the wave of variation I-A, a noncoherence arises between compositions I and A (Figures 5a and 5b). This noncoherence is resolved into a

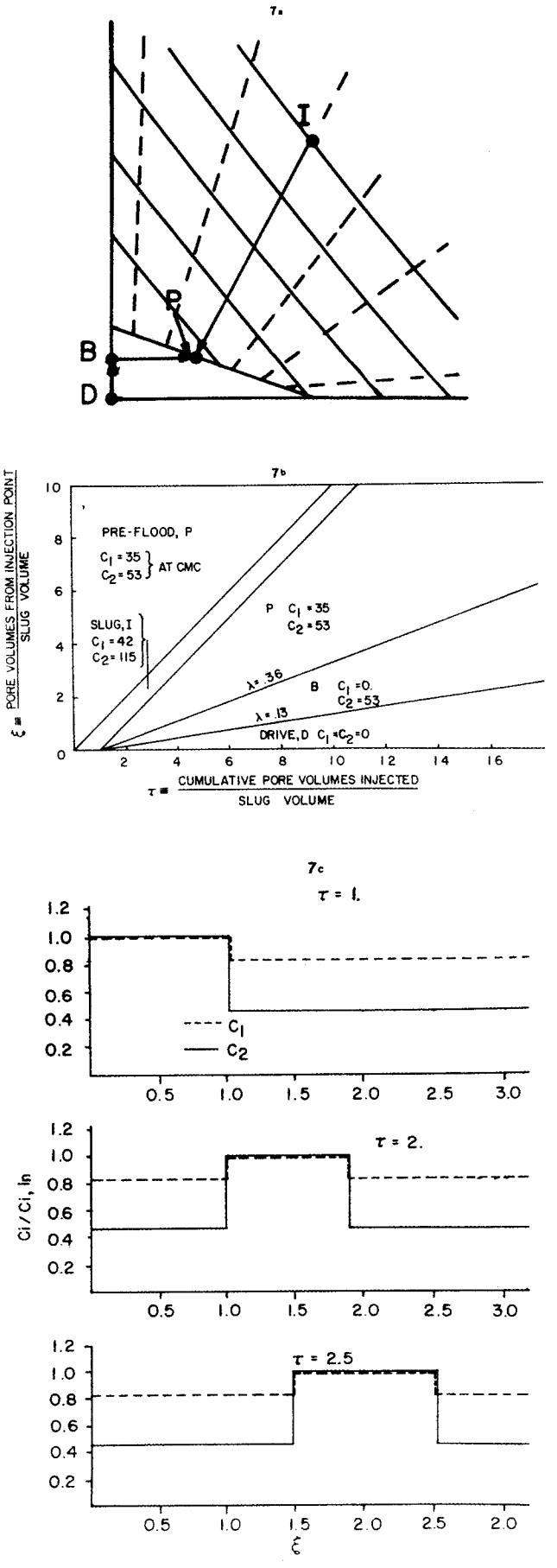

Figure 7. Use of a surfactant preflood. Pulse of mixed micelles in equilibrium with upstream concentrations propagates through the column at the bulk fluid velocity. (a) Schematic of composition route development (b) Distance-time diagram (c) Column profiles.

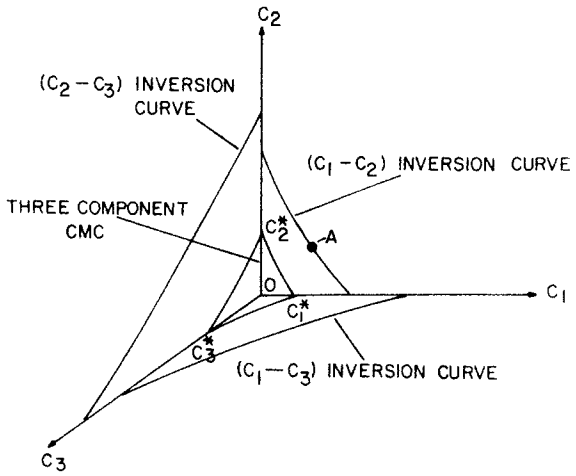

Figure 8. Outstanding features of the coordinate space of the dependent variables for a three-component system obeying the Trogus adsorption model.

spreading wave (Figure 5a 2) and an indifferent wave. The plateau composition is D. The indifferent wave of variation D-A travels at $\Lambda = 1$, and so quickly interferes with the wave of variation A-0. Composition D is coherent with composition 0, and produces a single slow shock of velocity $\Lambda = 0.314$. This shock has a lower velocity than the upstream spreading wave of variation C-D. As the shock interferes with the spreading wave, both the shock velocity and the composition variation across the shock (D'-E') change continuously. The shock velocity and the variation across the shock can be calculated exactly from a material balance across the shock and the compositions and composition velocities of the spreading wave. However, since the velocity of the shock will decrease from its initial value of 0.314 to 0.130, a reasonable approximation can be obtained from using an average velocity to find the point at which the interference is completed. The final pattern will be two pulses of the separated surfactants at concentrations below the CMC (Figure 5c).

Note that although the patterns of interference differ greatly between case 2 and case 3, the final result is the same: separation of the slug into components at concentrations below the CMC. This is a result of the assumption that only the monomer adsorbs. To oversimplify, if micelles do not absorb, micelles cannot desorb, and the final pattern after all possible interferences have occurred shows only concentrations below the CMC.

Case 4: Surfactant in Drive Solution

In enhanced oil recovery it may be desirable to maintain surfactant solutions at the injected concentrations for as long as possible, constrained, of course, by economic realities. The results shown in Figure 6 indicate that nothing is gained by use of surfactant in the drive fluid. In this case, the composition of the surfactant drive solution, 0′, has been selected so that it lies at the intersection of the CMC curve and the fast path passing through the slug composition, I. Because the two compositions lie on the same path, the wave between them is coherent and thus does not break up into two waves. However, the single wave does move at unit velocity, rapidly overtaking the slow wave at the slug front. Thus, adding surfactant to the drive solution does not help prevent slug degradation. Wave-wave interferences rapidly squeeze the surfactant concentrations down to values less than the CMC, where separation of the surfactant mixture is fastest.

Case 5: Surfactant Preflood

Preflooding with a surfactant solution having the same monomer concentrations as the slug *does* prevent slug degradation. The results shown in Figure 7 indicate that a preflood with a dilute so-

lution on the CMC curve, P, having the same monomer concentrations as the slug, I, will permit the slug to propagate unchanged. This result is a consequence of the phase separation model assumed here, but is independent of the form of the adsorption isotherms.

GENERALIZATIONS FOR n-COMPONENT SYSTEMS

A brief study of three-component systems will serve to clarify the logic by which the conclusions arrived at for two-component systems can be generalized for greater numbers of components. The inversion curve, discussed above, which arises in two-component systems when $K_1 < K_2$ and $C_1^* > C_2^*$, is the key to making these generalizations.

In the three-component case, the space of the dependent variables is three-dimensional (Figure 8). The CMC is now a surface rather than a curve. If the coherence condition is used to construct composition paths, there will be three families of paths. These paths will now be space curves. As a result, a representation corresponding to the composition path grid used in the two-component case would be difficult to obtain. However, each coordinate plane in Figure 8 will contain the composition path grid of the corresponding two-component system. Thus, each coordinate plane will contain an inversion curve, as defined above. This is illustrated in Figure 8. Furthermore, if two compositions which are represented by points in the same coordinate plane are in contact, the number of waves which will arise, the velocities of these waves, and the compositions between the waves may be predicted from the two-component path grids. This is true regardless of whatever other compositions are present in the rest of the system. As an example, if at a point in time compositions A and 0 in Figure 8 are in contact any place in a three-component system, with A upstream of 0, only one wave will result from that contact. That wave, between compositions A and 0, will be self-sharpening, and its velocity can be calculated from a material balance across the wave.

In order to extend our ability to predict the behavior of a three-component system, we next justify the assertion that there must exist in the space of the dependent variables "inversion surfaces" similar to the "inversion curves" of the two-component system. The inversion curve divides the two-component composition space into two regions. In one region the partition coefficient of component 2, $\overline{C}_2/C_2$, is greater than that of 1, $\overline{C}_1/C_1$; in the other, the opposite is true:

$$\text{Region } I: \frac{\overline{C}_2}{C_2} > \frac{\overline{C}_1}{C_1} \quad \text{Region } II: \frac{\overline{C}_2}{C_2} < \frac{\overline{C}_1}{C_1}$$

The retardation of a component by the substrate is directly related to its partition coefficient. The larger the partition coefficient, the greater the retardation. So, in Region I, component 2 is more strongly retarded than component 1; in Region II, the opposite is true, that is, component 1 is more strongly retarded. As stated above, the necessary and sufficient condition for an inversion curve to exist in a Trogus system is

$$K_2 > K_1$$
$$C_2^* < C_1^*$$

At low micelle concentrations, $K_2 > K_1$ results in $\overline{C}_2/C_2 > \overline{C}_1/C_1$. But if the total micelle concentration becomes great enough, then $C_2^* < C_1^*$ results in the preferential incorporation of so large a fraction of component 2 into the micelles, which do not absorb, that now $\overline{C}_2/C_2 < \overline{C}_1/C_1$.

Application of this same physical argument to the three-component case where

$$K_1 < K_2 < K_3 \tag{17}$$

$$C_1^* > C_2^* > C_3^* \tag{18}$$

indicates that the three-component composition space must also contain regions where relative magnitudes of partition coefficients change from region to region.

TABLE 3. GENERALIZATION OF EFFECTS OF MICELLE FORMATION TO n-COMPONENT SYSTEMS

Number of Components	Equation of Unit Velocity Paths	Number of Possible Inversions of Sequences of Partition Coefficients	Equations of Figures Separating the Regions of Different Sequences
2	line in two-space	1	curve in two-space
3	line in three-space	3	surface in three space
4	line in four-space	6	volume in four-space
n	line in n-space	$\frac{n^2-n}{2}$	$(n-1)$ dimensional hypervolume in n-dimensional hyperspace

These observations lead to the following conclusions regarding a three-component Trogus system which satisfies Eqs. 17 and 18.

1) Near the three-component CMC, the sequence in which the components will appear is:

1, 2, 3

2) As total concentration defined as

$$C = C_1 + C_2 + C_3$$

increases, the sequence of emergence will change in one of the following two manners:

	Sequence
Type I System	*Type II System*
1, 2, 3	1, 2, 3
2, 1, 3	1, 3, 2
2, 3, 1	3, 1, 2
3, 2, 1	3, 2, 1

3) The unit-velocity paths observed in the two-component case also arise in the three-component case. Though no longer restricted to the coordinate planes, they will still be straight lines. This is a consequence of the use of the phase separation model.

4) The composition paths below the CMC remain orthogonal owing to the assumption of Henry's Law.

The results of the above study of a three-component Trogus system are generalized to the case of an n-component system in Table 3.

SUMMARY AND CONCLUSIONS

1) The effects of the formation of mixed micelles on the chromatographic movement of mixed surfactants has been demonstrated by solution of the Trogus Model for a two-component system.

2) All the salient effects of micellization are demonstrated by the two-component case.

3) When it is true of a Trogus system that

$$C_1^* > C_2^* > \ldots > C_n^*$$

and

$$K_1 < K_2 < \ldots < K_n$$

then there will exist $[(n^2-n)/2] + 1$ composition regions in the coordinate space of the dependent variables separated by $(n^2-n)/2$ inversion loci. In each of the regions the order of retardation of the components will be different.

4) One of the most important aspects of finite surfactant slug behavior is determined by the existence of loci of constant monomer concentrations. Any two compositions connected by one of

these lines will give rise to an indifferent wave moving at the bulk fluid velocity.

5) Fractionation of surfactant slugs due to preferential adsorption may be eliminated by use of a preflood having the same monomer concentration as the slug. The micellar pseudophase will then propagate at the bulk fluid velocity because it will already be at equilibrium with the adsorbed concentrations downstream.

ACKNOWLEDGMENT

The authors wish to extend special thanks to Shell Development Company for making it possible for one of the authors (F. G. Helfferich) to participate in this study. Their encouragement and support during the initial stages of the work is recognized.

The research was supported by the Department of Energy (Phil Lorenz, Technical Project Officer) and by the following companies: Gulf Research and Development Co.; Chevron Oil Field Research, LaHabra, CA; Continental Oil Co.; Shell Oil's Bellaire Research Center, Houston, TX; Amoco Production Co., Tulsa, OK; Sun Oil Co., Richardson, TX; Witco Chemical Corp., Petrolia, PA; Mobil Research and Development, Dallas, TX; Exxon Production Research, Houston, TX; Stepan Chemical Co., Northfield, IL; Union Oil of California, Brea, CA; Elf Aquitaine, Pau, France; Texaco's Bellaire Research Laboratories, Houston, TX; and Marathon Research, Denver, CO.

NOTATION

c_i = moles of i in fluid phase/m^3 of fluid
C_i = moles of i in fluid phase/m^3 of column ($C_i = \phi c_i$)
$C_{i,d}$ = moles of i as monomer (disperse phase)/m^3 of column
$C_{i,\text{in}}$ = surfactant concentration at inlet
$C_{i,m}$ = moles of i in micellar form/m^3 of column
$C_{i,o}$ = initial surfactant concentration
$C_{i,t}$ = total concentration of i, moles of i/m^3 of column ($C_{i,t} = C_i + \overline{C}_i = C_{i,m} + C_{i,d} + \overline{C}_i$)
$\overline{C}_i$ = moles of i adsorbed/m^3 of column ($\overline{C}_i = (1-\phi)q_i/\hat{\rho}_s$
c_i^* = pure component CMC in absence of added electrolyte (moles of i/m^3 of fluid)
CMC = concentration of surfactant at which micelles begin to form according to the pseudophase separation model of Mysels and Otter
$\Delta\overline{C}_i$ = [$\overline{C}_i$ behind a shock] − [$\overline{C}_i$ ahead of the shock]
ΔC_i = [C_i behind a shock] − [C_i ahead of the shock]
k_i = Henry's Law constant (moles of i adsorbed per kg of substrate)/(mole of i per m^3 of fluid)
K_i = Henry's Law constant (dimensionless) $K_i = k_i\rho_s(1-\phi)/\phi$
q_i = adsorbed concentration of component i (moles of i adsorbed/kg of substrate)

Greek Letters

$\alpha_{i,j}$ = $\equiv [C_i^*/C_j^*]^\theta$
θ = empirical constant used to predict multicomponent CMCs (dimensionless)
λ = eigenvelocity of a wave defined by Eq. 12
ξ = dimensionless distance, (pore volumes from injection point)/(slug volume)
$\hat{\rho}_s$ = solid phase density (kg/m^3)
τ = dimensionless time, (pore volumes injected)/(slug volume)
ϕ = column void fraction (m^3 of fluid phase)/(m^3 of column)

LITERATURE CITED

Clint, J. H., "Micellization of Mixed Nonionic Surface Active Agents," *J. Chem. Soc.*, Faraday Trans. **I**, **71**, 1327 (1975).

Fernandez, M. E., "Adsorption of Sulfonates from Aqueous Solutions onto Mineral Surfaces," University of Texas M.S. Thesis (Dec., 1978).

Helfferich, F. G., "General Theory of Multicomponent, Multiphase Displacement in Porous Media," SPEJ, **21**, (1), p 51 (1981).

Helfferich, F. G., and G. Klein, *Multicomponent Chromatography: Theory of Interference*, Marcel Dekker, Inc., New York (1970).

Lake, L. W., and G. W. Pope, "Status of Micellar-Polymer Field Tests," *Pet. Eng. Int.*, **51**, 13, p. 38 (1979).

Mysels, K. J., and R. J. Otter, "Thermodynamic Aspects of Mixed Micelles," *J. Colloid Sci.*, **16**, 474 (1961).

Rubingh, D. N., "Mixed Micelle Solutions," *ACS Colloid Surface Sci. Symp.*, 52nd (Knoxville), **1**, 185 (1978).

Scamehorn, J. F., "Equilibrium Adsorption of Surfactants on Mineral Oxide Surfaces from Aqueous Solutions," University of Texas Ph.D. Dissertation (May, 1980).

Trogus, F. J., R. S. Schechter, G. A. Pope, and W. H. Wade, "Adsorption of Mixed Surfactant Systems," *J. of Pet. Tech.*, p. 769, *J. Pet. Tech.* (June, 1979a).

Trogus, F. J., W. H. Wade, and R. S. Schechter, "A New Interpretation of Adsorption Maxima and Minima," *J. of Colloid and Interface Sci.* **70**, 8, 293 (1979b).

Manuscript received August 29, 1980; revision received July 13, and accepted August 7, 1981.

APPENDIX

Analysis for a Binary Surfactant System

Because the computational procedure is based on an established approach very few mathematical details have been presented in the body of the paper. The physical interpretation of the results was viewed as the essential issue; however, it may be useful to consider an outline of the procedure to better appreciate the results.

The concentration velocity expressed by Eq. 13 is also given by the following

$$V_{c_i} = -\left(\frac{\partial C_{i,T}}{\partial t}\right)_z \Big/ \left(\frac{\partial C_{i,T}}{\partial z}\right)_t = -\left(\frac{\partial C_i}{\partial t}\right)_z \Big/ \left(\frac{\partial C_i}{\partial z}\right)_t \tag{18}$$

Substituting the material balance equation and noting that by definition the composition velocities are all equal for a coherent wave, then

$$\left(\frac{\partial C_{i,T}}{\partial z}\right)_t = +\frac{1}{\lambda}\left(\frac{\partial C_i}{\partial z}\right)_t \tag{19}$$

and

$$\left(\frac{\partial C_{i,T}}{\partial t}\right)_z = \frac{1}{\lambda}\left(\frac{\partial C_i}{\partial t}\right)_z \tag{20}$$

where

$$\lambda = \frac{V_{ci}}{V} = \frac{V_{cj}}{V} \qquad \text{for } i = 1,\ldots n$$

If $C_{i,T}$ is regarded as a function of the solution concentration, C_i, a consequence of assuming local equilibrium, then

$$dC_{i,T} = \sum_{j=1}^{n} \frac{\partial C_{i,T}}{\partial C_j}\, dC_j = \sum_{j=1}^{n} m_{i,j}\, dC_j \tag{21}$$

Of course, $C_{i,T}$ is a function of a position and time so that we also have

$$dC_{i,T} = \left(\frac{\partial C_{i,T}}{\partial z}\right)_t dz + \left(\frac{\partial C_{i,T}}{\partial t}\right)_z dt \tag{22}$$

But from Eqs. 19 and 20 it is seen that

$$dC_{i,T} = \frac{1}{\lambda}\left(\frac{\partial C_i}{\partial z}\right)_t dz + \frac{1}{\lambda}\left(\frac{\partial C_i}{\partial t}\right)_z dt = \frac{1}{\lambda}\, dC_i$$

Equation 21 can, therefore, be expressed in the form

$$dC_i = \lambda \sum_{j=1}^{n} m_{i,j}\, dC_i \tag{23}$$

In matrix form for a binary system

$$\begin{bmatrix} \lambda m_{1,1} - 1 & \lambda m_{1,2} \\ \lambda m_{2,1} & \lambda m_{2,2} - 1 \end{bmatrix} \begin{bmatrix} dC_1 \\ dC_2 \end{bmatrix} = \begin{bmatrix} 0 \\ 0 \end{bmatrix} \tag{24}$$

The characteristic equation giving the eigenvalues for Eq. 24 is

$$(\lambda m_{1,1} - 1)(\lambda m_{2,2} - 1) - m_{1,2}\, m_{2,1}\, \lambda^2 = 0$$

which yields

$$\lambda = \frac{m_{1,1} \pm ((m_{1,1} - m_{2,2})^2 + 4 m_{1,2}\, m_{2,1})^{1/2}}{2(m_{1,1}\, m_{2,2} - m_{1,2}\, m_{2,1})} \tag{25}$$

and the eigenvectors are

$$\frac{dC_1}{dC_2} = \frac{\lambda m_{1,2}}{1 - \lambda m_{1,1}} \tag{26}$$

In order to construct a composition path in the $(C_1 - C_2)$-plane, one chooses a composition near the boundary, then evaluates Eqs. 25 and 26 from the definitions of the $m_{i,j}$ and the relations

$$C_{i,t} = \overline{C}_i + C_i$$

$$\overline{C}_i = K_i\, C_{i,d}$$

$$\phi \sum C_{i,d} = \left[\frac{(\Pi \phi C_i^*)^\theta}{\sum x_i \left(\prod_{i \neq j} \phi C_j^* \right)^\theta} \right]^{1/\theta}$$

$$\frac{C_{1,m}}{C_{2,m}} = \frac{C_{1,d}}{C_{2,d}} \left(\frac{C_2^*}{C_1^*} \right)^\theta$$

This system is highly nonlinear, so that the values of the $m_{i,j}$ must be evaluated numerically (e.g., by Newton's method) and Eq. 26 must be integrated numerically for each eigenvalue, as, for example, in this work, the Runge-Kutta-Gill algorithm was used.

As noted in the body of the paper, when the eigenvelocities along a composition path decrease in the direction of flow, as, for example, in Figures 4a and 5a which correspond to cases 2 and 3, the composition paths constructed as above no longer describe the system behavior. This is because the shock wave that arises in the column presents a discontinuity across which Eq. 6 no longer applies. The wave velocity and composition of the intermediate zone can no longer be determined from the composition path grid. However, a simple mass balance across the shock front yields the relation

$$V_{c_i} = \frac{V}{1 + \dfrac{\Delta \overline{C}_i}{\Delta C_i}} \tag{27}$$

for a coherent shock we still require that

$$V_{c_i} = V_{c_2}$$

Equation 27 must be solved by trial and error to obtain $\Lambda = V_{c_i}/V$ and the composition of the intermediate zone. In case 3, Figure 5 a1, it can be seen that composition A, the intermediate composition arising between the injected composition I and the original composition 0, is only slightly off the composition path through I. In this case, the composition obtained from constructing the composition route without accounting for shock formation is only slightly in error. However, in figure 4 a1, the composition B obtained from Eq. 27 differs considerably from the composition which would be obtained by following the composition paths. This is because of the presence of the CMC discontinuity across the composition path.

Dynamic Contact Angles

E. B. GUTOFF
and C. E. KENDRICK
Polaroid Corp. Waltham, MA 02254

The dynamic contact angles of various liquids on a gelatin-subbed polyester tape were investigated by plunging a tape into a pool of liquid, in the manner of Perry and of Burley and Kennedy. The effect of the upper fluid was studied by replacing the air normally present by immiscible oils. A fair correlation was found at the point of air entrainment, relating the capillary number, $\mu V/\sigma$, to a physical properties number, $g\mu^4/\rho\sigma^3$. A dimensional correlation, relating the air entrainment velocity to the viscosity to the −0.67 power, was even better. At various velocities, the dynamic contact angle (or the dynamic contact angle minus the static angle) could be related to the capillary number, the physical properties number, and to density and viscosity ratios. Again, the dimensional correlations were better than the dimensionless ones, perhaps caused by an omission of a significant dimensionless group due to our inability to choose a suitable characteristic length.

With any one system, the data could be expressed as $\theta = kN_{Ca}^b$ above some minimum velocity, or, covering all velocities, as $(\theta - \theta_s) = kN_{Ca}^b$. With air as the upper fluid, all the data at one angle lie within one decade, with capillary numbers at air entrainment in the range of 0.6–1.3.

SCOPE

In most coating operations the coating solution forms a dynamic contact line with the moving base, with air as the third phase. The maximum coating speed is often limited to that base velocity at which air is entrained by the moving base into the coating solution. At that point the dynamic contact angle reaches 180°. This study extends the work of Burley and Kennedy (1976b, 1978) and Perry (1967) on the effect of fluid properties and base velocity on dynamic contact angles, by plunging a gelatin-subbed polyester tape into various liquids. The effect of the third phase, usually air, was studied by replacing the air with immiscible oils.

As there is no readily accessible characteristic length, only two dimensionless ratios of forces can be involved. By dimensional analysis the dynamic contact angle should be correlated with the capillary number, $N_{Ca} = \mu V/\sigma$, a physical properties number, $N_{pp} = g\mu^4/\rho\sigma^3$, and ratios of the physical properties of two fluids, and perhaps to the static contact angle.

ISSN-0001-1541-82-4437-0459-$2.00.